Introducing composite lattice core sandwich structure as an alternative proposal for engine hood

Sha Yin[a,b,c], Haoyu Chen[a,b], Yaobo Wu[a,b], Yibing Li[d], Jun Xu[a,b,c,d,*]

[a] *Department of Automotive Engineering, School of Transportation Science and Engineering, Beihang University, Beijing 100191, China*
[b] *Advanced Vehicle Research Center (AVRC), Beihang University, Beijing 100191, China*
[c] *State Key Laboratory for Strength and Vibration of Mechanical Structures, School of Aerospace Engineering, Xi'an Jiaotong University, Xi'an 710049, China*
[d] *State Key Laboratory for Automotive Safety and Energy, Tsinghua University, Beijing 100084, China*

ABSTRACT

Pedestrian protection capability is critical for lightweight design of automotive engine hood. Here, a novel and lightweight composite sandwich hood including two fiber reinforced composite panels and a lattice core was proposed and the corresponding pedestrian protection performance was evaluated via Head Injury Criterion (HIC). The novel double-curvature composite sandwich hood with a pyramidal lattice core was designed based on a commercialized product with a weight reduction by 25%, and fabricated using interlocking approach. A homogenized constitutive model was developed for the pyramidal lattice core and utilized in the following headform-to-hood impact simulations with LS-DYNA. The stiffer sandwich hood revealed better pedestrian safety performance compared with the corresponding baseline hood without lattice core where secondary collision happened. Also, effects of geometrical variables, material selection and core types were discussed. The variation of panel thickness played a more important role in the average HIC values compared with that of core geometries. Among various material selections, hoods designed with carbon fiber reinforced composite (CFRC) panels and a flax fiber reinforced composite (FFRC) lattice core achieved the minimum head injury. Additionally, lattice core outperformed traditional honeycomb and foam in sandwich hood design. The present study demonstrates the feasibility of employing lattice materials in lightweight design of hood and other car body coverage.

1. Introduction

In vehicle-to-pedestrian accidents, head trauma is one of the fatal damage forms and head injuries account for 31.4% of 3305 Abbreviated Injury Scale (AIS) 2+ injuries [1]. Statistics show that the impact on front side of cars is the major cause of pedestrian deaths (83.5%) [2]. Automotive hood and windshield are frequent pedestrian head injury sources and should be designed for pedestrian safety [3,4]. A well-designed hood can modify the acceleration response of head impact and thus mitigate head injury [5]. Pedestrian impact tests are performed according to regulations provided by Euro NCAP (European New Car Assessment Programme) and HIC value is commonly used as the criterion to evaluate the severity of a possible head injury. Wu and Beaudet proposed an ideal acceleration-time history waveform peaking rapidly and decaying exponentially to achieve HIC < 1000 [6].

Energy and environment sustainability restricts the development of traditional automotive industry. Lightweight design, including lightweight materials selection and structural optimization, has become a

hot topic to solve these problems [7]. Fiber composite material has shown greater specific properties with respect to their metallic counterparts such as aluminum and steel commonly used in traditional car body, and has attracted lots of attentions of OEM (Original Equipment Manufacturer). Moreover, sandwich structures consisting of two face sheets and a low-density core (such as honeycomb and foam core), are also popular in car body for lightweight design and crushing protection [8]. Several studies have been dedicated to the new design concepts of hoods based on pedestrian protection behavior. For example, previous research showed that the average HIC values of carbon fiber composite hoods were lower than those of steel and aluminum hoods [9]. Zhou et al. focused on sandwich hood and proposed an novel corrugated core hood design [10]. Peng et al. also evaluated the integral stiffness and pedestrian protection behavior of sandwich hoods with a honeycomb core [11].

Architected materials, as known as lattice materials, were termed as the most potential lightweight material of the next generation because of their high structural efficient and multi-functional advantages

* Corresponding author at: Department of Automotive Engineering & Advanced Vehicle Research Center (AVRC), Beihang University, Beijing 100191, China.
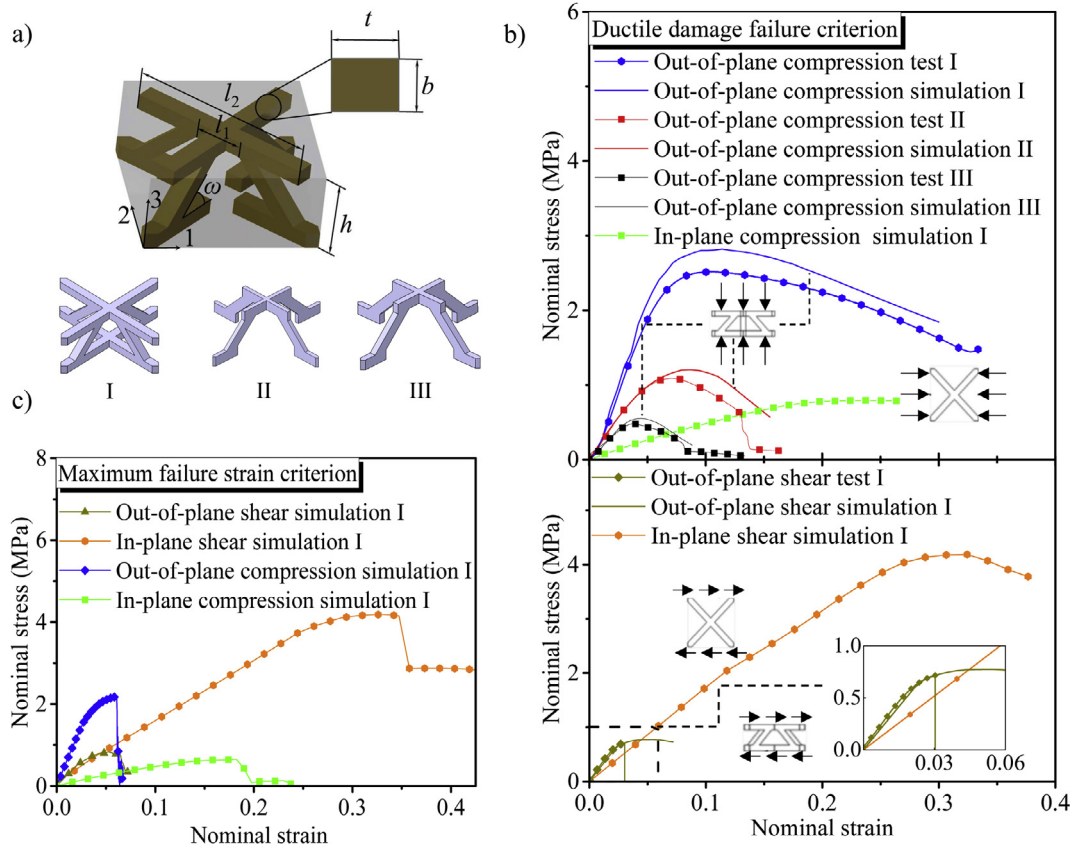 *E-mail address:* junxu@buaa.edu.cn (J. Xu).

Fig. 1. a) Schematic of a pyramidal lattice unit cell with controllable geometric parameters and models of three design points I to III in Ref. [24]; b) stress-strain curves of pyramidal lattice unit cells under compression and shear loading condition by experiments and simulation with ductile damage failure criterion; c) stress-strain curves of unit cell analysis with maximum failure strain criterion.
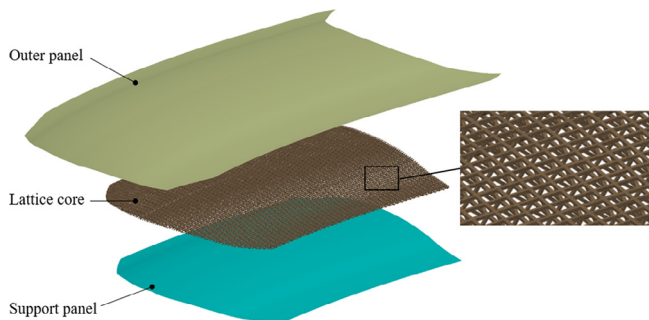

Fig. 2. Exploded view of lattice core sandwich hood.

[12,13]. Some composite structures, such as liquid filled lattice structures [14,15] and soft energy absorption structures [16] were proved to possess good energy absorption capability. Crashworthiness of fiber reinforced composite lattice structure was also investigated in the previous literature [17]. Numerical methods including homogenization modeling [18,19] and detailed modeling methods [20] were proposed to accurately evaluate the mechanical properties. Pyramidal lattice, for example, showed their excellent mechanical properties together with energy absorption capability at ultra-low density [21], which could be promising for vehicle lightweight applications. Interlocking approach has been used to construct a single-curvature lattice structure, and pyramidal lattice cylinders shell has been investigated [22,23]. Additionally, a low-cost and recyclable approach by employing natural flax fiber as reinforcement in the lattice materials was investigated by Gao et al. [24]. FFRC could be a cheap and eco-friendly choice for automotive hood manufacturing [25].

The aim of this study is to evaluate the pedestrian protection capability of a novel lattice core sandwich hood. The sandwich hood containing a composite pyramidal lattice core was designed and fabricated using interlocking approach. Subsequently, headform-to-hood impact simulations were conducted according to Euro NCAP standard [26]. Effects of material selection and geometrical variables were also discussed for head injury mitigation strategies and further hood design guidance.

2. Lattice material modeling

For a lattice core sandwich hood, the detailed explicit model contains approximately 6000 representative volume elements (RVE), which is computationally prohibitive and time-consuming to regenerate the entire model when local designs change. In the present study, a homogenization method for lattice materials will be utilized referring to previous studies [27,28]. The lattice geometry is simplified into an equivalent continuum which replicates the volumetric average stress and strain fields under general loading conditions. Thus, the simulation results will only contain volumetric average terms but not the field variation within each individual lattice truss member, which will greatly simplify large-scale structural analysis of lattice materials.

2.1. Constitutive model of lattice material

The pyramidal lattice materials have special symmetry as shown in Fig. 1 and can be termed orthotropic which have nine independent elastic constants. The elastic constitutive function of pyramidal lattice can be described as Eqs. (1) and (2) with elastic strain tensor and stress tensor (with Cartesian indices):
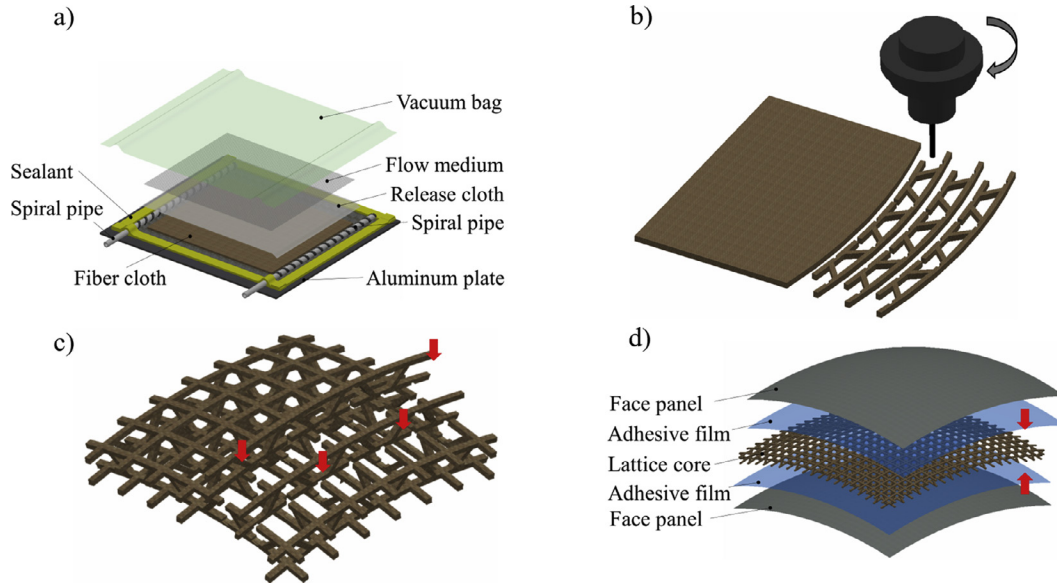
Fig. 3. The fabrication flowchart of the double-curvature lattice sandwich structures: a) processing composite sheets using VARI method; b) truss strips cutting from composite sheet; c) assembled double-curvature lattice core; d) sandwich panels.
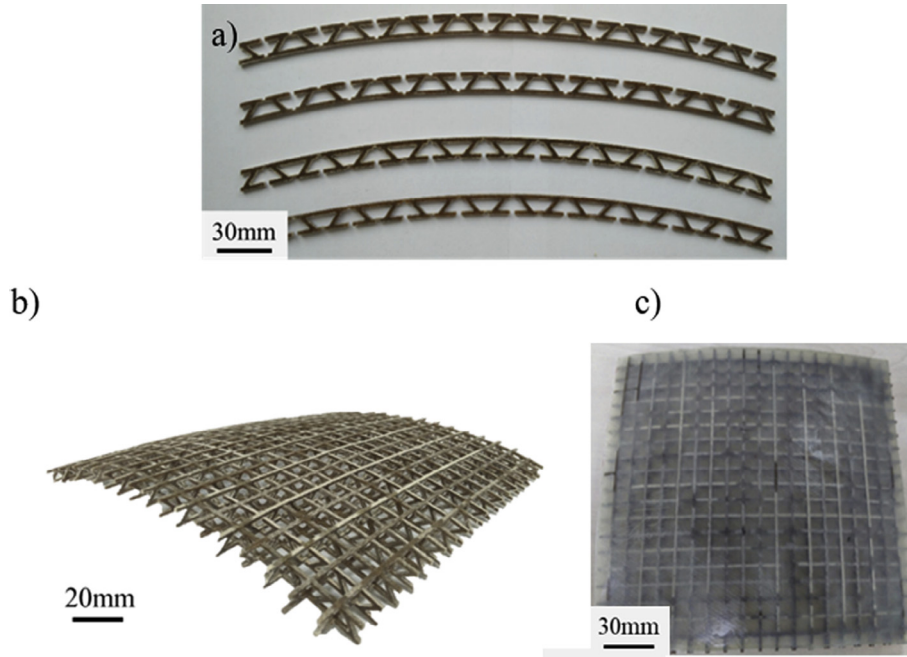

Fig. 4. Double-curvature pyramidal lattice sandwich structure: a) interlocking strips; b) lattice core and c) sandwich panel.

$$
\begin{Bmatrix} \varepsilon_1 \\ \varepsilon_2 \\ \varepsilon_3 \\ \varepsilon_4 \\ \varepsilon_5 \\ \varepsilon_6 \end{Bmatrix} = \begin{bmatrix} S_{1111} & S_{1122} & S_{1133} & 0 & 0 & 0 \\ S_{2211} & S_{2222} & S_{2233} & 0 & 0 & 0 \\ S_{3311} & S_{3322} & S_{3333} & 0 & 0 & 0 \\ 0 & 0 & 0 & S_{2323} & 0 & 0 \\ 0 & 0 & 0 & 0 & S_{1313} & 0 \\ 0 & 0 & 0 & 0 & 0 & S_{1212} \end{bmatrix} \begin{Bmatrix} \sigma_1 \\ \sigma_2 \\ \sigma_3 \\ \sigma_4 \\ \sigma_5 \\ \sigma_6 \end{Bmatrix}
\tag{1}
$$

where the elastic compliance matrix S_{ij} can be given with engineering elastic constants as:

$$
S = \begin{bmatrix} 1/E_1 & -v_{12}/E_2 & -v_{13}/E_3 & 0 & 0 & 0 \\ & 1/E_2 & -v_{23}/E_3 & 0 & 0 & 0 \\ & & 1/E_3 & 0 & 0 & 0 \\ & & & 1/G_{23} & 0 & 0 \\ & \text{sym.} & & & 1/G_{31} & 0 \\ & & & & & 1/G_{12} \end{bmatrix}
\tag{2}
$$

2.2. Lattice material properties

According to the constitutive equation above, nine independent elastic constants are necessary to describe the elastic response of homogenized lattice material (E_{11}, E_{22}, E_{33}, G_{12}, G_{31}, G_{23}, v_{12}, v_{31}, v_{32}), which can be gained by uniaxial testing, meso-mechanics analysis, numerical simulation and combination thereof [27]. Thus, four types of
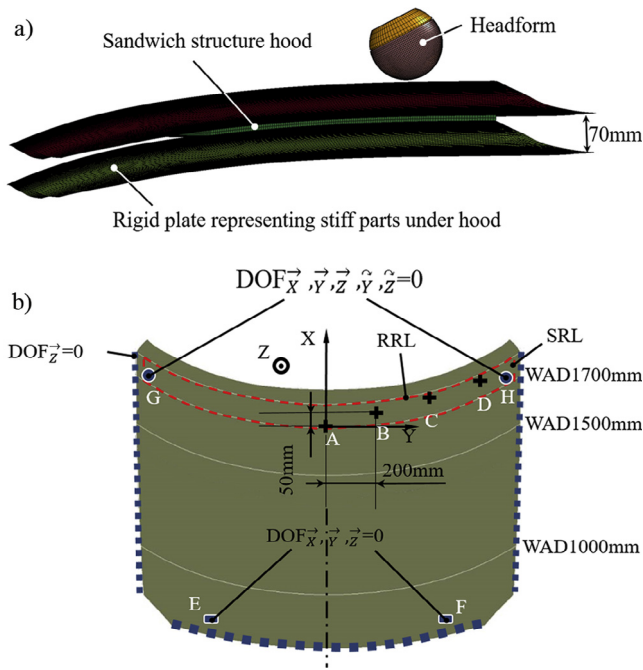
Fig. 5. a) Headform-to-hood FEA impact model; b) illustration of boundary conditions and impact locations.

uniaxial tests including in-plane compression, in-plane shear, out-of-plane compression and out-of-plane shear needed to be carried out as clarified in Fig. 1b). Here, unit cell (Fig. 1) modeling was adopted in ABAQUS/CAE to acquire these constants, with geometrical parameters strut inclination $\omega = 45°$, length between two inclined struts at the pyramidal node $l_1 = 6.34$ mm, height of lattice structure $h = 10$ mm, width of struts $b = 2$ mm and thickness of interlocking stripes $t = 2.4$ mm. The mechanical properties of flax fiber reinforced composites were obtained from the previous literature [24]. Ductile damage failure criterion was employed and then the corresponding failure strain gained from the stress-strain curves was input. During the unit cell analysis, the free sides of the unit cell were simply supported. The mechanical responses of the unit cell lattice under different loading conditions were shown in Fig. 1b), Also, Poisson's ratios in three principle axes could also be obtained with the same unit cell in free boundary conditions. The resultant modulus shows good agreement with the theoretical predictions in the Ref. [24].

The modeling results above were validated by comparison against experimental tests including out-of-plane compression and shear, as compared in Fig. 1b). The experimental setup and specimen of through-thickness compression tests follows the standard [29]. Out-of-plane shear tests are performed on a hydraulic servo testing machine (MTS 810) using single-arm shear clamp at a displacement rate of 1 mm/min following ASTM C273. Samples with 3×6 unit cells were prepared, and at least two repeated tests are carried out to ensure the repeatability. The stiffness and strength values by modeling are 4.1% and 10% greater comparing with experiments, which is acceptable. Accordingly, the properties obtained from unit cell simulation will be used as input in the following analysis.

3. Design and modeling of engine hood

3.1. Design

For a commercialized engine hood, the integral surface consists of several double-curvature sections separated by character lines. Based on a commercialized engine hood, a double-curvature sandwich hood was further designed with profiling smoothed and localized curvature

variation ignored as shown in Fig. 2, which was composed of an outer panel, a pyramidal lattice core and a support panel with thickness of 2.5 mm, 10 mm and 2.5 mm, respectively. Note that the coverage area of the lattice core and support panel was limited to adult and child head impact area according to Euro NCAP standard, and the unfilled space under the outer panel is occupied by hinges and latch mechanisms attached. The hood panels were fabricated with 12 plies of carbon fiber weave fabric. A typical sandwich hood weighs 12.97 kg, achieving a weight reduction of 25% compared to the mass of the commercialized steel hood (17.30 kg).

A cost- and time-efficient fabrication method is vital for the application of the above designed sandwich hood. In this work, the interlocking process developed in the former publication [24,30,31], was employed for a double-curvature pyramidal lattice core sandwich panel. The whole fabrication flowchart was illustrated in Fig. 3. Firstly, flax fiber reinforced laminates were fabricated based on vacuum assisted resin infusion (VARI) method as specified in Gao's work [24]. Secondly, strips with shape designed according to the curvature of panels were cut off from the laminates by engraving machine and then grooved in for the following assembly. Then, the strips were interlocked and assembled in proper order forming the double-curvature pyramidal lattice cores. Finally, the outer and support panels fabricated with glass fiber reinforced composites (for the visibility of lattice cores inside) by VARI approach were bonded to the lattice cores using adhesive films. The fabricated strips, pyramidal lattice core and sandwich panel were shown in Fig. 4. The overall size of the double-curvature sandwich panel was about 300 mm × 300 mm × 35 mm weighing only 319.12 g. Note that the fabrication approach proposed is also feasible for any arbitrary double-curvature lattice core sandwich panels and hoods thereof.

3.2. Modeling

3.2.1. Homogenization method validation

To validate the continuum homogenization approach, low velocity impact (LVI) models were built up in LS-DYNA according to a testing procedure ASTM D7136/D7136M [32]. As shown in Fig. 6a) and b), finite element (FE) models of square sandwich plates with detailed 6×6 lattice unit cells and the corresponding homogenized models were established, respectively. Three groups of lattice geometric parameters are considered: I). b/h = 0.2, t/h = 0.24, II). b/h = 0.16, t/h = 0.16 and III). b/h = 0.225, t/h = 0.2. Eight-node solid elements are used for detailed and homogenized lattice core and Belytschko-Tsay shell elements for the face sheets. An hourglass model with an hourglass coefficient of 0.05 and control type 5 is utilized in detailed and homogenized lattice core which are with solid section. The sandwich panels were fully constrained at the four boundaries in LVI test. The detailed lattice model directly utilized the raw material mechanical properties as input, while for homogenized lattice core, the mechanical properties (nine elastic constants, stress-strain curves and failure strain) obtained from unit cell analysis aforementioned as shown in Fig. 1b) were imported into MAT40 NONLINEAR_ORTHOTROPIC. A hemispherical impactor with a mass of 3.215 kg and radius of 10.25 mm was applied and the impact velocity was set to be 2.5 m/s to acquire a kinetic energy of 10 J. The acceleration and kinetic energy variation of impactors were recorded and compared between two modeling approaches in Fig. 6c)~e). Although the detailed numerical model predicts an undulatory acceleration value than the simulation results for homogenized models, tendency of the two simulating methods are virtually the same, and the average level can be considered as a good correlation. Therefore, the homogenization method in this study is reliable for the following modeling about impact tests of lattice core sandwich hoods.

3.2.2. Sandwich hood modeling

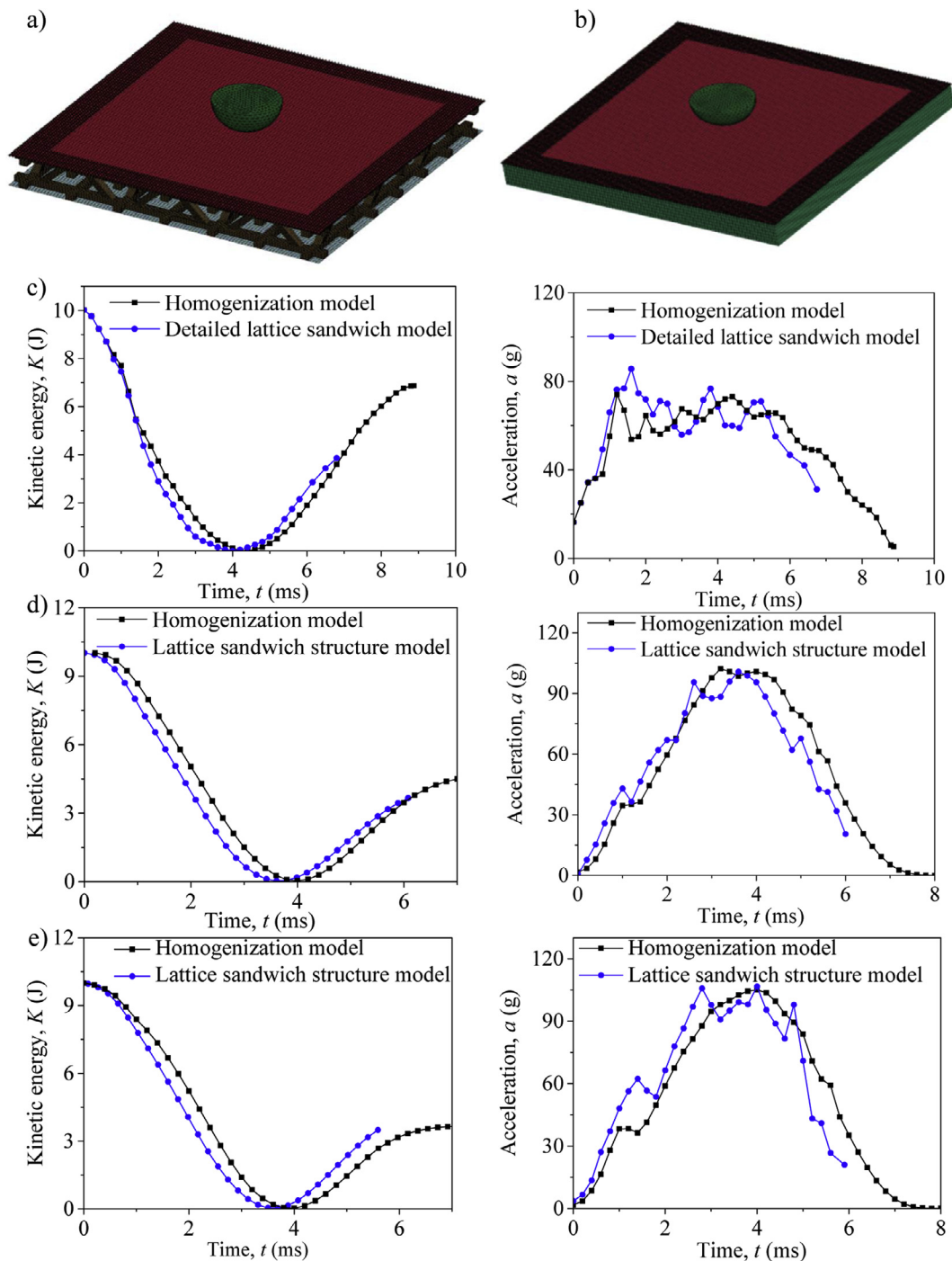To evaluate the pedestrian protection capability of lattice core

Fig. 6. Comparison between the detailed lattice sandwich model and homogenized model: a) detailed lattice sandwich LVI model; b) homogenized lattice sandwich LVI model; c), d) and e) are comparison of kinetic energy-time and acceleration-time histories between two models for geometric parameter group I), II) and III).

sandwich hoods, a headform-to-hood impact model was established in LS-DYNA according to Euro NCAP standard as illustrated in Fig. 5. As EEVC standard recommends, an underhood clearance of 70 mm can guarantee the minimum HIC value under 800. Thus, a rigid surface parallel to the outer hood surface with a translational distance of 70 mm was created representing the stiff parts under the engine hood (*e.g.* engine block) as shown in Fig. 5a [33]. An adult head FE model which has been validated otherwise was employed in this study. The headform contains 5 parts weighing 4.8 kg, including a null shell, an outer shell with viscoelastic property, an aluminum inner shell, an aluminum baseplate and an accelerometer. One may refer to [9] for more details about the headform modeling. Referring to the impact

configurations of Euro NCAP adult headform tests, the headform was launched against the impact hood at a speed of 40 km/h with an impact angle of 65° to the ground reference level. As shown in Fig. 5b, four impact points A-D were selected from the red-dot-line area amongst wrap around distance (WAD) 1700 mm, the rear reference line (RRL) and side reference lines (SRL) with X and Y coordinate values incremented by 50 mm and 200 mm respectively. At the latch positions (Pointes E and F), all translational degrees of freedom (DOFs) were constrained; while at hinge positions (Points G and H), all DOFs were fixed except the rotational DOF in XOZ plane. Displacement in Z direction was constrained for the leading and lateral edges of hoods.

The hood outer and support panels were defined as shell elements
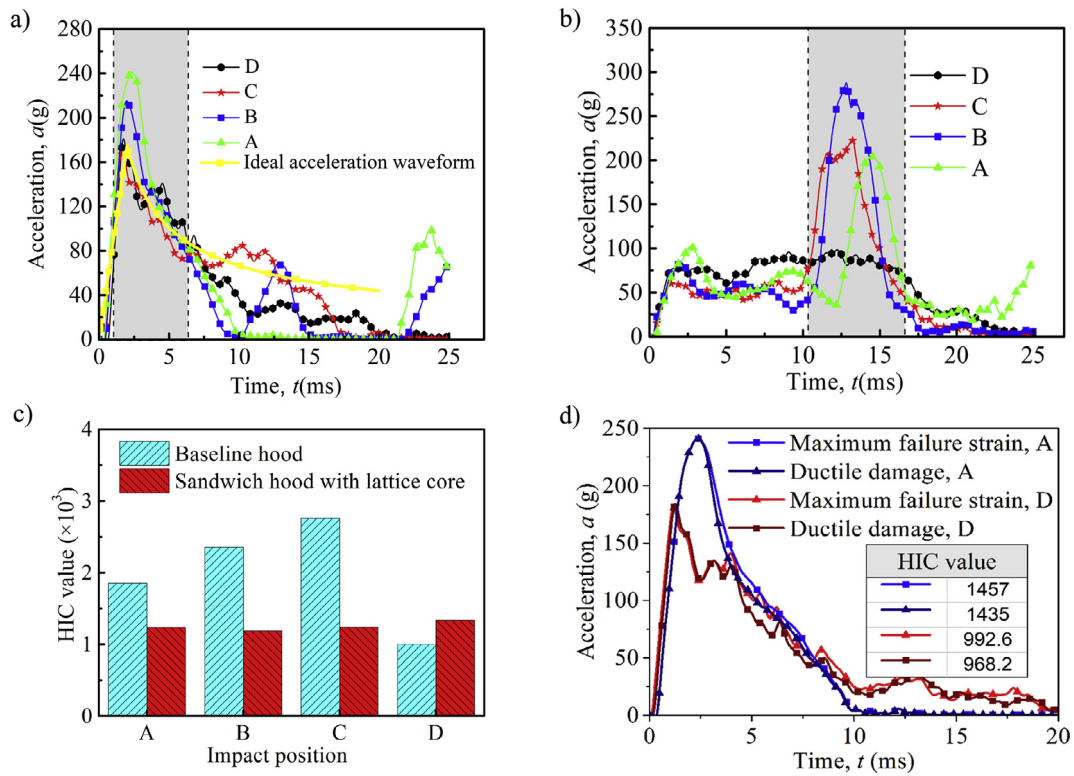
Fig. 7. Resultant acceleration-time curves: a) lattice core sandwich hood and b) baseline hood (shadow areas indicate the time phase of acceleration peaks); c) summary of the resultant HIC values of baseline hood and sandwich hood at 4 impact locations; d) result comparison at impact points A and D between two head-to-hood impact simulations with different failure criterions during unit cell analysis.

(S4R) while the homogenized lattice core was constructed of solid elements (C3D8R). The three layers were connected by setting as conode to simulate the interfacial properties between each two neighboring layers. Finally, the sandwich hood impact model shown in Fig. 5 was simulated with 205,201 shell elements and 90,978 solid elements. MAT40 material model utilized in Section 3.2.1 was again employed here for flax fiber reinforced composite lattice core after homogenization, and MAT54/55 COMPOSITE_DAMAGE for twelve plies of carbon fiber fabric composite hood panels with Chang-Chang failure criterion automatically executed.

To investigate the effect of lattice core on the pedestrian protection capability of engine hood, the same impact simulation of a baseline hood without lattice cores was carried out for comparison. The baseline hood with lattice core removed is a double-layer shell structure similar to most commercialized hoods composed of outer and support panels. The boundary conditions were set to be the same, while additionally displacement in Z direction was constrained for the two lateral boundaries of isolated support panel.

3.3. HIC calculation

Head Injury Criterion (HIC) proposed by the National Highway Traffic Safety Administration (NHTSA) is defined as Eq. (3):

$$HIC = \max_{t_1 < t_2, t_2 - t_1 \leqslant 15ms} \left\{ \left[1/(t_2 - t_1) \int_{t_1}^{t_2} a(t)/g \, dt \right]^{2.5} (t_2 - t_1) \right\} \tag{3}$$

The equation shows that HIC value is an integration value of acceleration during a limited time (HIC$_{15}$ corresponding to 15 ms). Once a headform impact simulation is executed, the resultant HIC$_{15}$ value could be calculated automatically from the acceleration-time (a-t) curve through 1000 Hz SAE filter in the post-treatment module of LS-DYNA. When HIC$_{15}$ value surpasses the threshold of 1000, the collision is deemed to bring irreversible injury to an adult head.
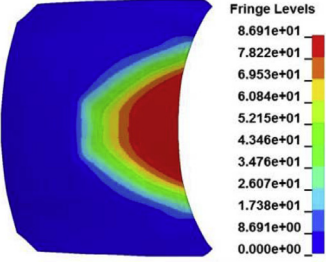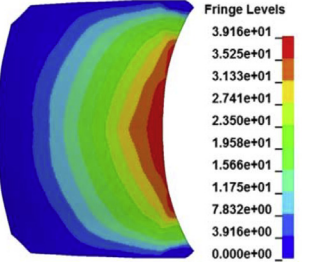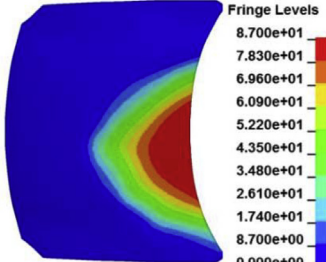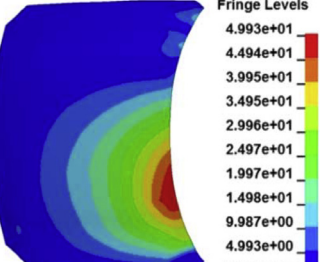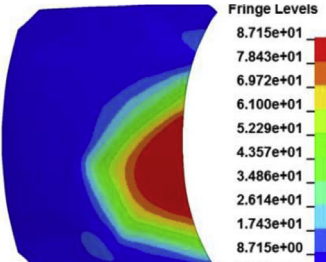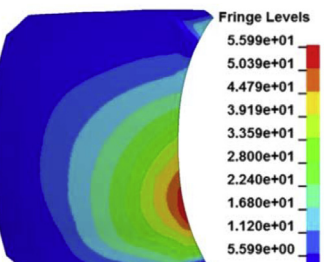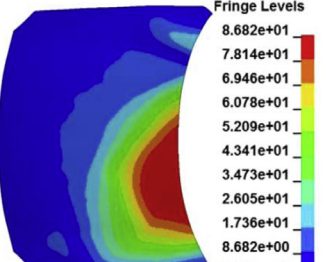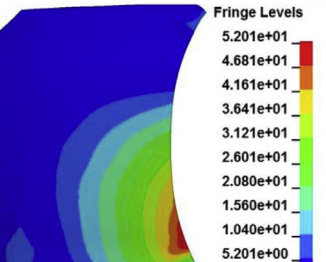
A typical acceleration response curve is consisted of four phases, the peaks of which are dominated in sequence by hood active mass, hood stiffness, boundary condition and secondary collision, respectively [34]. Among the four factors, structural stiffness and secondary collision will significantly affect the hood average HIC value. The acceleration ascends with hood stiffness; on the other hand, large deformation for a relatively soft hood or impact upon stiff under-hood parts will possibly induce a secondary collision which arouses a high peak value of acceleration as well. Accordingly, an appropriate integral stiffness will be vital for the design of a pedestrian-friendly hood.

4. Result and discussion

4.1. Pedestrian protecting performance

In order to evaluate the pedestrian protecting performance of lattice core sandwich hood, the corresponding acceleration responses and HIC values on four impact locations were compared with those of baseline hood as shown in Fig. 7. The acceleration-time curve of sandwich hood as shown in Fig. 7a contains one major peak at ~2 ms without significant peaks afterwards. The first peak is due to active mass and structural stiffness which dissipate most of the kinetic energy. Note that the resultant a-t curves of sandwich hood are rather similar to the ideal one from Wu and Beaudet [6]. Compared to sandwich hood, the a-t curves of baseline hood are quite different. Taking the response at impact point B as an example shown in Fig. 7b, the initial a-t curve of baseline hood is relatively flat and the major peak appears at ~12 ms (with duration time about 6 ms) which reflects severe secondary collision induced by the large deformation of baseline hood at impact point, as illustrated in the contour of Table 1. Secondary collision results in higher HIC values of baseline hood. The impact a-t curves at points A and C are quite similar with that at point B but different from that at point D. The impact point D is close to hinges where large deformation

Table 1
Deformation contours in four impact locations (A-D) and the corresponding HIC values.

Impact locations	Lattice core Sandwich hood	Baseline hood
A	$HIC_{15} = 1236$	$HIC_{15} = 1851.6$
B	$HIC_{15} = 1189$	$HIC_{15} = 2851.4$
C	$HIC_{15} = 1237$	$HIC_{15} = 2759$
D	$HIC_{15} = 1336$	$HIC_{15} = 878$

is constrained and thus no secondary collision happens. According to the acceleration–time waveforms, the HIC values of sandwich hood at four impact points were summarized and compared with those of baseline hood in Fig. 7c. The average HIC value of sandwich hood decreases noticeably by 40% comparing with that of baseline hood, with total weight increase of only 2.1% for the existence of core. Besides,

head-to-hood impact simulations with different failure criterion during analysis of unit cell are carried out. The corresponding acceleration-time curves as well as HIC values at impact points A and D show good agreement (Fig. 7d), which proves that the failure criterion during analysis of unit cell has little influence on the evaluation of pedestrian protection capability.

Table 2
Parametric matrix of geometric variables of lattice core sandwich hoods.

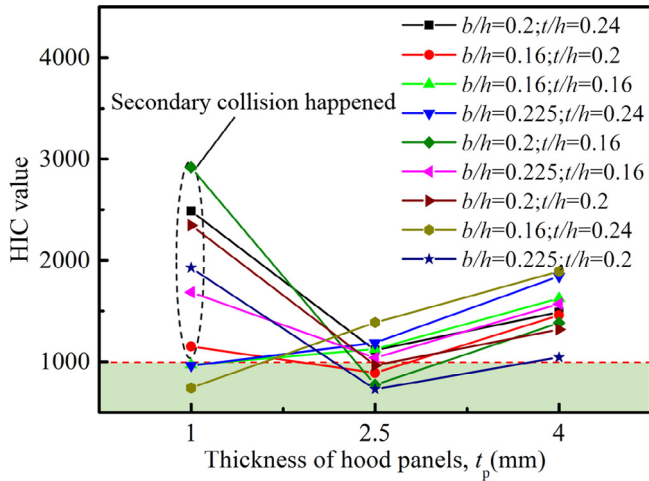| b/h	t/h	t_p (mm)
0.16	0.16	1
0.2	0.2	2.5
0.225	0.24	4

Fig. 8. Resultant HIC values with different t_p at different combinations of b/h and t/h.
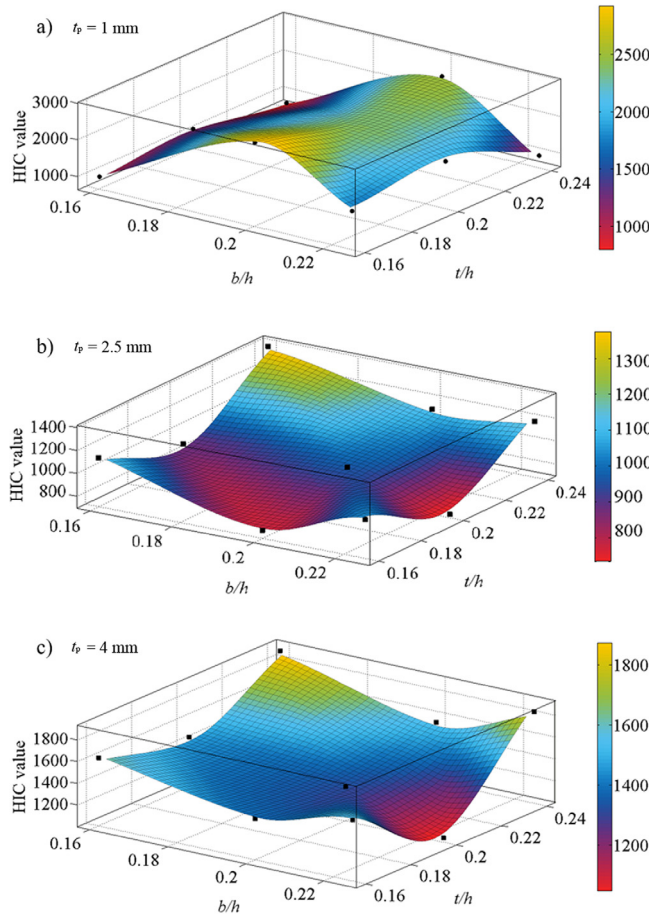

Fig. 9. HIC variation tendencies with b/h and t/h at different t_p: a) $t_p = 1$ mm; b) $t_p = 2.5$ mm; c) $t_p = 4$ mm.

4.2. Effects of geometric variables

One advantage of lattice core sandwich hoods is their designability with various variables either in panels or lattice cores. The panel thickness t_p, and two dimensionless variables b/h and t/h were taken as geometric variables with l_1 fixed to 6.34 mm and inclination angle $\pi/4$ suggested by the previous work [35]. For each variable, three values were given as shown in Table 2 and all the variables were fully coupled. Then, hood FE model were created and simulated for 27 possible combinations in total. Headform was also launched against impact hood at four impact points A-D, and the corresponding a-t curves were recorded. The average HIC values of four impact points with various t_p are plotted in Fig. 8 at different b/h and t/h. Generally, the average HIC values decrease first and then increase with hood panel thickness, and $t_p = 2.5$ mm is the most satisfactory parameter in terms of pedestrian protection. As $t_p = 2.5$ mm, about half of the designed combinations meet HIC < 1000 threshold. As hood thickness increases from 2.5 mm to 4 mm, the stiffness increases and thus the resistance to impact deformation increases. According, the headform acceleration increases resulting in higher HIC values for $t_p = 4$ mm. On the other hand, as hood thickness decreases from 2.5 mm to 1 mm, secondary collision is ready to happen with a relatively soft hood which causes resultant HIC values over 1100. When the secondary collisions tend to happen in virtue of lower hood stiffness or lack of underhood clearance, adjustment of lattice geometric parameters may change hood stiffness and eliminate secondary collisions as shown in Fig. 8.

The effects of lattice core geometries b/h and t/h to HIC value is limited as shown in Fig. 8 and more explicit tendencies about core geometries to the HIC value at different panel thickness are plotted in Fig. 9. The average HIC value will increase first and then decrease with b/h and t/h when panel thickness $t_p = 2.5$ mm and 4 mm with none secondary collision scenarios, and thus a combination of b/h and t/h corresponding to the minimum HIC value is recommended for lattice core design; while for $t_p = 1$ mm, the tendency is completed reversed.

The mass of sandwich hoods with carbon fiber reinforced composite panels and flax fiber reinforced lattice core at different panel thicknesses and core geometries was calculated and summarized in Table 3. Variation of panel thickness plays a more significant role on the hood mass than that of lattice core geometries. The hood mass fluctuation with t_p increased by 1.5 mm is approximately 6.8 kg while that with lattice geometric variables rarely surpasses 2 kg.

4.3. Effects of material variables

To investigate effects of material types, headform-to-hood impact tests for a series of material combinations of sandwich hood as summarized in Table 4 have been simulated with panel thickness fixed at 2.5 mm, $b/h = 0.225$ and $t/h = 0.2$. CFRC (TORAY T700SC-12K weave fabric), glass fiber reinforced composite (GFRC) (3238A/EW250F) and FFRC (fabricated in laboratory) were selected as raw materials of both hood panel and lattice cores for comparison and the corresponding mechanical properties were shown in Table 5. Besides, other core materials such as PMI foam (ROHACELL®200WF) and aluminum honeycomb were also examined here with the same core height. Honeycomb and PMI material were separately modeled using MAT_HONEYCOMB and MAT_SOIL_AND_FOAM, with referred input parameters [36].

Fig. 10 illustrates the pedestrian protection capability versus hood mass at different material combinations standing from different points of view. As shown in Fig. 10a, hoods with FFRC panels occupy higher HIC and lighter weight area, while those with CFRC and GFRC panels possess acceptable HIC and greater weight areas. The HIC values of CFRC panels are generally lower than those of GFRC ones. From the viewpoint of core material shown in Fig. 10b, HIC values of lattice cores are generally lower than those of foam and honeycomb. Note that the materials property variation of foam and honeycomb is limited in this study, however, the results indicate that sandwich hoods with PMI foam

Table 3
Mass of lattice core sandwich hoods (kg) with different geometric variable combinations.

b/h	t/h	Hood mass at different t_p (kg)		
		$t_p = 1$ mm	$t_p = 2.5$ mm	$t_p = 4$ mm
0.2	0.24	6.89	13.75	20.61
0.16	0.2	7.10	13.96	20.82
0.225	0.16	6.83	13.69	20.55
0.2	0.2	6.31	13.17	20.03
0.16	0.16	6.72	13.58	20.44
0.225	0.24	7.96	14.82	21.68
0.2	0.16	6.12	12.98	19.84
0.16	0.24	7.94	14.80	21.66
0.225	0.2	7.12	13.98	20.84

Table 4
Material variable combinations of lattice core sandwich hoods.

No.	Core material	Hood panel material
1	CFRC	CFRC
2	GFRC	GFRC
3	FFRC	CFRC
4	FFRC	FFRC
5	FFRC	GFRC
6	PMI foam	CFRC
7	PMI foam	FFRC
8	PMI foam	GFRC
9	Aluminum honeycomb	CFRC

Table 5
Mechanical properties of raw material in lattice structures and hood panels.

CFRC			
ρ (kg/m^3)	1500	σ_{11}^t (MPa)	912
E_{11}(MPa)	55,779	σ_{11}^c (MPa)	708
E_{22}(MPa)	54,572	σ_{22}^t (MPa)	771
ν_{12}	0.4	σ_{22}^c (MPa)	698
G_{12}(MPa)	4214	τ_{12}^s (MPa)	132
GFRC			
ρ (kg/m^3)	1900	σ_{11}^t (MPa)	505
E_{11}(MPa)	24,500	σ_{11}^c (MPa)	380
E_{22}(MPa)	24,500	σ_{22}^t (MPa)	505
ν_{12}	0.42	σ_{22}^c (MPa)	380
G_{12}(MPa)	34,100	τ_{12}^s (MPa)	55
FFRC			
ρ (kg/m^3)	1180	σ_{11}^t (MPa)	35
E_{11}(MPa)	2500	σ_{11}^c (MPa)	90
E_{22}(MPa)	2500	σ_{22}^t (MPa)	35
ν_{12}	0.4	σ_{22}^c (MPa)	90
G_{12}(MPa)	2070	τ_{12}^s (MPa)	38

and honeycomb may have comparable pedestrian protection capability, but still inferior to those with lattice cores. Compared with the commercial steel hood aforementioned, there are noticeable mass reductions as well as pedestrian protection capability improvement for the lattice core sandwich hood. Furthermore, the best material combination corresponding to the lowest HIC value from Fig. 10 should be CFRC panels and FFRC lattice cores with ideal lightweight effects as well.

5. Conclusion

A novel lattice core sandwich hood was developed in the present study for automotive lightweight and the pedestrian protection capability was examined. The double-curvature sandwich hood consisting of two fiber reinforced composite panels and a pyramidal lattice core was designed based on a commercial product, and its weight can be reduced by 25% comparing with that of the steel commercial one. Interlocking fabrication method was employed to realize the above
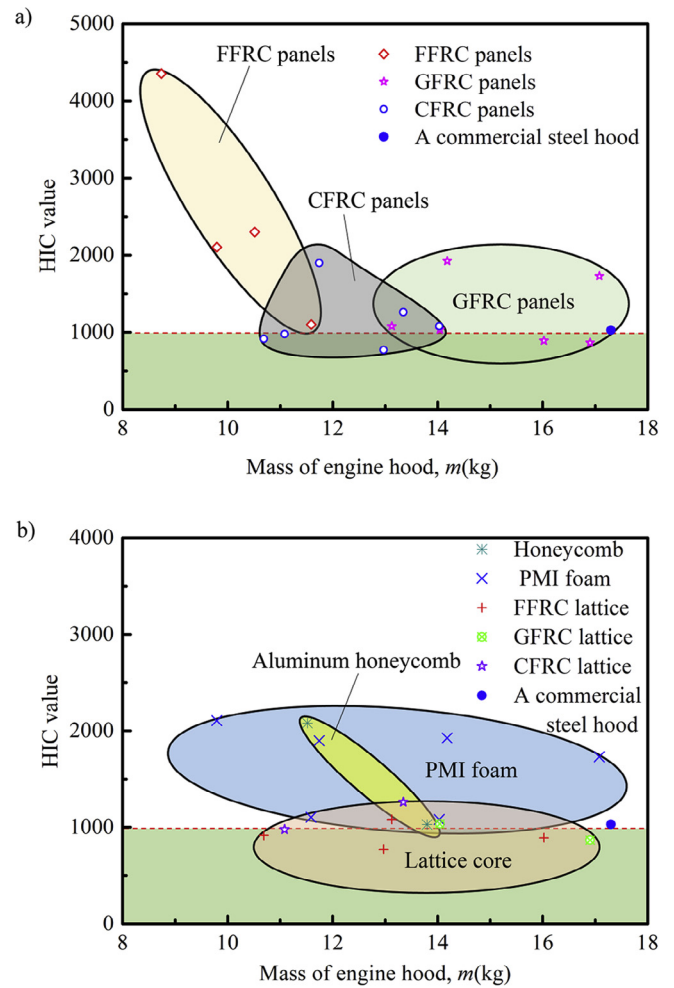

Fig. 10. Ashby style plot of pedestrian protection capability and lightweight effect of material variables analysis results in the light of a) panel materials and b) core materials.

design. The pedestrian protection performance of sandwich hoods was evaluated via HIC value of headform through headform-to-hood impact tests. A homogenized constitutive model was developed for the pyramidal lattice core and utilized in the following impact simulations with LS-DYNA. Referring to the impact configurations of the Euro NCAP adult headform tests, the headform was launched against the impact hood and four impact points were selected from the specified area. The resultant a-t curves of sandwich hood were rather similar to the ideal one from literature [6]. Also, the stiffer sandwich hood design showed better pedestrian safety performance compared with the corresponding baseline hood without lattice core.

Effects of geometrical variables, material selection and core types were discussed. The overall bending stiffness of sandwich hood to some extent determines the corresponding pedestrian protection performance. The average HIC values varies more significantly with panel thickness than core geometries. Among various material selections, hood designed with carbon fiber reinforced composite (CFRC) panels and a flax fiber reinforced composite (FFRC) lattice core achieved the minimum head injury. Moreover, lattice core outperformed traditional honeycomb and foam core in the sandwich hood design. The present work demonstrates the feasibility by employing lattice core materials in hood design. The relatively complete methodology on how to efficiently simulate complex sandwich structures would benefit future car-body lightweight design.

Acknowledgement

References

[1] Yoshiyuki M. Summary of IHRA pedestrian safety WG activities (2005) – proposed test methods to evaluate pedestrian protection afforded by passenger cars, Proceedings of the 19th International Technical Conference on the Enhanced Safety of Vehicles. Washington DC, 2005.

[2] NCSA data resource website, fatality analysis reporting system (fars) encyclopedia, National Highway Traffic Safety Administration, 2015. https://www.fars.nhtsa.dot.gov/People/PeoplePedestrians.aspx.

[3] Xu J, Li YB, Chen X, Ge DY, Liu BH, Zhu MY, et al. Automotive windshield—pedestrian head impact: energy absorption capability of interlayer material. Int J Auto Technol 2011;12:687–95.

[4] Liu BH, Zhu MY, Sun YT, Xu J, Ge DY, Li YB. Investigation on energy absorption characteristics of PVB laminated windshield subject to human head impact. Appl Mech Mater 2010;34–35:956–60.

[5] Zhou J, Wang F, Wan X. Optimal design and experimental investigations of aluminum sheet for lightweight car hood. Mater Today Proc 2015;2:5029–36.

[6] Wu J, Beaudet B. Optimization of head impact waveform to minimize HIC. In: Proceedings of the SAE world congress & exhibition. 2007.

[7] Kaluza A, Kleemann S, Fröhlich T, Herrmann C, Vietor T. Concurrent design & life cycle engineering in automotive lightweight component development. Procedia Cirp 2017;66:16–21.

[8] Velea MN, Wennhage P, Zenkert D. Multi-objective optimization of vehicle bodies made of FRP sandwich structures. Compos Struct 2014;111:75–84.

[9] Torkestani A, Sadighi M, Hedayati R. Effect of material type, stacking sequence and impact location on the pedestrian head injury in collisions. Thin Wall Struct 2015;97:130–9.

[10] Liu Q, Xia Y, Zhou Q. Design analysis of a sandwich hood structure for pedestrian protection. Gener Moto Res Dev 2009;09:0356.

[11] Peng Y, Han Y, Chen Y, Yang J, Willinger R. Assessment of the protective performance of hood using head FE model in car-to-pedestrian collisions. Int J Crash 2012;17:1–9.

[12] Vaziri A, Xue Z, Hutchinson JW. Metal sandwich plates with polymer foam-filled cores. J Mech Mater Struct 2006;1:97–127.

[13] Deshpande VS, Fleck NA, Ashby MF. Effective properties of the octet-truss lattice material. J Mech Phys Solids 2001;49:1747–69.

[14] Liu Y, Schaedler TA, Jacobsen AJ, Lu W, Qiao Y, Chen X. Quasi-static crush behavior of hollow microtruss filled with NMF liquid. Compos Struct 2014;115:29–40.

[15] Liu Y, Wang L. Enhanced stiffness, strength and energy absorption for co-continuous composites with liquid filler. Compos Struct 2015;128:274–83.

[16] Zhou J, Deng X, Yan Y, Chen X, Liu Y. Superelasticity and reversible energy absorption of polyurethane cellular structures with sand filler. Compos Struct 2015;131:966–74.

[17] Sebaey TA, Mahdi E. Crushing behavior of a unit cell of CFRP lattice core for sandwich structures' application. Thin Wall Struct 2017;116:91–5.

[18] Deng X, Zhang C, Chen Y, Yan Y, Liu Y, Chen X. Crush behaviors of polyvinyl chloride cellular structures with liquid filler. Compos Struct 2018;189:428–34.

[19] Liu X, Li M, Li X, Deng X, Zhang X, Yan Y, et al. Ballistic performance of UHMWPE fabrics/EAMS hybrid panel. J Mater Sci 2018;53:7357–71.

[20] Liu Y, Schaedler TA, Chen X. Dynamic energy absorption characteristics of hollow microlattice structures. Mech Mater 2014;77:1–13.

[21] Yin S, Wu L, Ma L, Nutt S. Hybrid truss concepts for carbon fiber composite pyramidal lattice structures. Compos Part B-Eng 2012;43:1749–55.

[22] Yang J, Xiong J, Ma L, Zhang G, Wang X, Wu L. Study on vibration damping of composite sandwich cylindrical shell with pyramidal truss-like cores. Compos Struct 2014;117:362–72.

[23] Xiong J, Ghosh R, Ma L, Vaziri A, Wang Y, Wu L. Sandwich-walled cylindrical shells with lightweight metallic lattice truss cores and carbon fiber-reinforced composite face sheets. Compos Part A-Appl Sci Manuf 2014;56:226–38.

[24] Xu J, Gao X, Zhang C, Yin S. Flax fiber-reinforced composite lattice cores: a low-cost and recyclable approach. Mater Des 2017;133:444–54.

[25] Kong C, Lee H, Park H. Design and manufacturing of automobile hood using natural composite structure. Compos Part B-Eng 2016;91:18–26.

[26] Euro NCAP Pedestrian Test Protocol v8.3, European New Car Assessment Programme, 2017. https://www.euroncap.com/en/for-engineers/protocols/pedestrian-protection/.

[27] Hundley JM, Clough EC, Jacobsen AJ. The low velocity impact response of sandwich panels with lattice core reinforcement. Int J Impact Eng 2015;84:64–77.

[28] Xue Z, Hutchinson JW. A comparative study of impulse-resistant metal sandwich plates. Int J Impact Eng 2004;30:1283–305.

[29] Committee CCMAD. Standard Test Method for Flatwise Compressive Properties of Sandwich Cores. C365/C365M-16. 2011.

[30] Russell B, Deshpande V, Wadley H. Quasistatic deformation and failure modes of composite square honeycombs. J Mech Mater Struct 2008;3:1315–40.

[31] Yin S, Wu L, Nutt S. Stretch–bend-hybrid hierarchical composite pyramidal lattice cores. Compos Struct 2013;98:153–9.

[32] ASTM D7136/D7136M-15, Standard Test Method for Measuring the Damage Resistance of a Fiber-Reinforced Polymer Matrix Composite to a Drop-Weight Impact Event, ASTM International, 2015.

[33] Qi L, Yong X, Qing Z. Friction effects in pedestrian headform impacts with engine hoods. J Thu Nat Sci 2009;14:631–8.

[34] Nie B, Zhou Q, Xia Y. Multi-peak characteristics of pedestrian head to automotive hood impact and structural design. Auto Saf Energy 2017;8(1):65–71.

[35] Deshpande VS, Fleck NA. Collapse of truss core sandwich beams in 3-point bending. Int J Solids Struct 2001;38:6275–305.

[36] Xie S, Zhou H. Analysis and optimisation of parameters influencing the out-of-plane energy absorption of an aluminium honeycomb. Thin Wall Struct 2015;89:169–77.